Evolution of A-Type Macrosegregation in Large Size Steel Ingot After Multistep Forging and Heat Treatment

ABDELHALIM LOUCIF, EMNA BEN FREDJ, NATHAN HARRIS,
DAVOOD SHAHRIARI, MOHAMMAD JAHAZI,
and LOUIS-PHILIPPE LAPIERRE-BOIRE

A-type macrosegregation refers to the channel chemical heterogeneities that can be formed during solidification in large size steel ingots. In this research, a combination of experiment and simulation was used to study the influence of open die forging parameters on the evolution of A-type macrosegregation patterns during a multistep forging of a 40 metric ton (MT) cast, high-strength steel ingot. Macrosegregation patterns were determined experimentally by macroetch along the longitudinal axis of the forged and heat-treated ingot. Mass spectroscopy, on more than 900 samples, was used to determine the chemical composition map of the entire longitudinal sectioned surface. FORGE NxT 1.1 finite element modeling code was used to predict the effect of forging sequences on the morphology evolution of A-type macrosegregation patterns. For this purpose, grain flow variables were defined and implemented in a large scale finite element modeling code to describe oriented grains and A-type segregation patterns. Examination of the A-type macrosegregation showed four to five parallel continuous channels located nearly symmetrical to the axis of the forged ingot. In some regions, the A-type patterns became curved or obtained a wavy form in contrast to their straight shape in the as-cast state. Mass spectrometry analysis of the main alloying elements (C, Mn, Ni, Cr, Mo, Cu, P, and S) revealed that carbon, manganese, and chromium were the most segregated alloying elements in A-type macrosegregation patterns. The observed differences were analyzed using thermodynamic calculations, which indicated that changes in the chemical composition of the liquid metal can affect the primary solidification mode and the segregation intensity of the alloying elements. Finite element modeling simulation results showed very good agreement with the experimental observations, thereby allowing for the quantification of the influence of temperature and deformation on the evolution of the shape of the macrosegregation channels during the open die forging process.

I. INTRODUCTION

THE presence of chemical heterogeneities and nonuniform distribution of alloying elements produced during solidification of metallic alloys is called segregation. Depending on its scale,[1] segregation can be observed at three levels: *microsegregation* takes place at the scale of dendrites, *macrosegregation* occurs at the scale of the product, and *mesosegregation* is produced at an intermediate scale such as primary grains. Macrosegregation is commonly observed in large size cast ingots. The typical macrosegregation patterns that could be formed in cast ingots are presented in Figure 1.[2,3] Depending on their position, morphology, and concentration, different patterns can be revealed: positive at the top, negative conic at the bottom, A-type bands (channels) between the centerline and the external surface, and V-type bands along the centerline of the ingot.[1,3] The A-type segregation bands appear as linear regions,[4] which present an important enrichment in alloying elements.[5] They are caused by the movement of enriched interdendritic fluid through the mushy zone as a result of thermosolutal convection.[6]

ABDELHALIM LOUCIF, EMNA BEN FREDJ, NATHAN HARRIS, DAVOOD SHAHRIARI, and MOHAMMAD JAHAZI are with the Département de Génie Mécanique, École de Technologie Supérieure, 1100, rue Notre-Dame Ouest, Montréal, QC, H3C 1K3, Canada. Contact email: abdelhalim.loucif.01@gmail.com LOUIS-PHILIPPE LAPIERRE-BOIRE is with Finkl Steel-Sorel, 100 McCarthy, Saint-Joseph-de-Sorel, QC, J3R 3M8, Canada.
Manuscript submitted September 9, 2017.
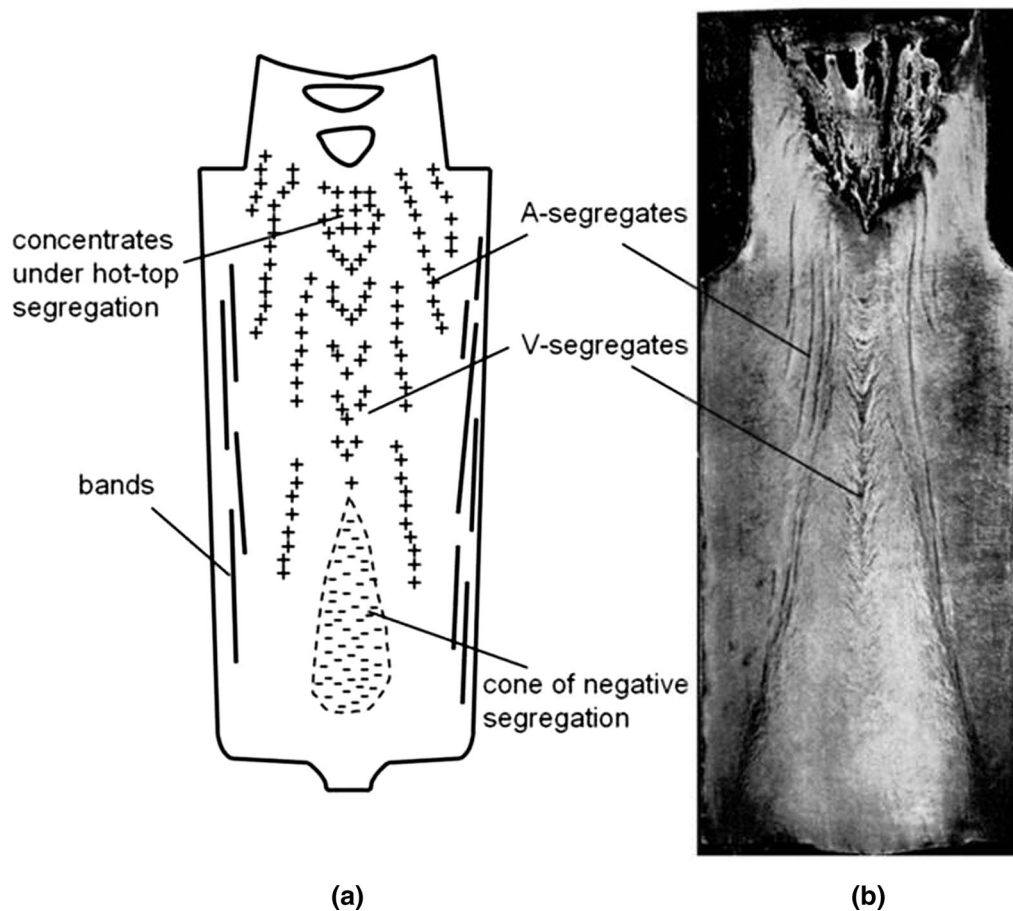Article published online March 30, 2018.

Fig. 1—Typical macrosegregation patterns that could be formed in steel ingots: (*a*) schematic representation and (*b*) sulfur print of a 10-ton ingot.[2,3] ("Mechanisms of Formation of A- and V-Segregation in Cast Steel," J.J. Moore and N.A. Shah: *J. Int. Met. Rev.*, copyright Institute of Materials, Minerals and Mining, reprinted by permission of Taylor & Francis Ltd., www.tandfonline.com on behalf of Institute of Materials, Minerals and Mining.).

Often, the as-cast steel ingots undergo open die forging operations at high temperatures for processing to final (shafts, rolls, and slabs) or semifinished products used as preforms for closed die forging. The ingots are generally preheated at high temperatures for long durations, often resulting in reduction or rarely in elimination of macrosegregation patterns. However, in large size high-strength steel ingots that contain significant amounts of alloying elements, some segregation, particularly macrosegregation, may still remain after the homogenization heat treatment.[7] On the other hand, it is well known that macrosegregation zones with their different chemical compositions modify the thermophysical properties[8] and microstructure[6] and may induce changes in the mechanical properties of the affected zones.[5] Higher homogenization temperatures or longer holding times are not viable alternatives because they increase the cost of the finished product and may also induce local melting, which leads to cracking during subsequent forging operations.[9]

Despite the fact that the physical principles of macrosegregation are known,[2] little information is available on the influence of processing conditions on the evolution of macrosegregation in large size ingots,

especially in the case of A-type segregation bands. However, in recent years, there has been significant demand for large size forged ingots of high-strength steels used in energy and transportation industries. Therefore, strong incentives exist for a better understanding of macrosegregation, its evolution, and its prediction after postcasting operations. A-type macrosegregation patterns in as-cast steels can be observed using a suitable solution containing hydrochloric[10] or nitric[11] acids. However, this method gives a general picture of the segregation state for all solute elements. Moreover, it is not possible to obtain information on the segregation characteristics of each alloying element. Differences in size, diffusivity, and thermodynamic properties of each solute element influence the extent and degree of macrosegregation. Cao *et al.*[11] analyzed the chemical composition of cubic samples taken from A-type bands in 27SiMn steel ingot. They revealed carbon, silicon, and manganese enrichment.

Macrosegregation chemical mapping would be the ideal way to characterize such enrichment. It can be determined by analyzing the chemical composition and distribution of each alloying element from the surface to

the center of the ingot with an appropriate step size. Very little data are available on chemical maps of alloying elements, especially in the case of large size steel ingots. In a recent work, Pickering et al.[12] constructed the chemical map, employing automated macroscale X-ray fluorescence spectroscopy in an as-cast 12 metric ton (MT) steel ingot. The chemical analyses were conducted in a slice that had been cut along the longitudinal axis of the ingot in steps of 5 mm in two perpendicular directions. They revealed the presence of A-type macrosegregation patterns. However, the work was limited to only two elements, chromium and molybdenum. Furthermore, Ge et al.[13] used finite volume simulation to study A-type macrosegregation in a 55 MT as-cast steel ingot. The simulation results were able to predict this type of chemical heterogeneity.

It is important to note that most of the experimental or simulation investigations on A-type macrosegregation in steel ingots were carried out in the as-cast state, i.e., just after solidification. Few studies are available in connection with the analysis of macrosegregation after forging and heat treatment operations. Such studies are very important, as they could indicate the effect of deformation and heat treatment on the evolution of segregation patterns and could be used as an evaluation criterion for the quality of the final products, particularly for critical components such as turbine shafts. Moreover, they would allow a better understanding of the fundamental mechanisms governing the behavior of A-segregation after casting, forging, and heat treatment processes.

In the present investigation, using a combination of macroetching, chemical analyses, and thermodynamic modeling, the distribution of the alloying elements present in the A-type macrosegregation bands in a forged and heat-treated 40 MT ingot was investigated and correlated with the segregation mechanisms. The evolution of macrosegregation bands during forging was also modeled using finite element simulation, and the results were interpreted in relation to the deformation processing conditions.

II. MATERIALS AND METHODS

The nominal chemical composition of the medium-carbon low-alloy steel used in this study is given in Table I. The casting was carried out in a 40 MT capacity cylindrical mold (eutectic gray iron) with solidification time of about 17 hours. After solidification and removal of the hot top, the diameters of the cast ingot and its height were 150 and 250 cm, respectively. The cast ingot was forged in parallelepiped form with final dimensions of $102 \times 127 \times 254$ cm^3 (Figure 2(a)) followed by quench and temper operations. A 2-cm-thick slice was cut along the longitudinal axis of the slab (Figure 2(a)) with the final dimensions of $2 \times 102 \times 254$ cm^3. For practical purposes, several rectangular blocks $2 \times 20 \times 38$ cm^3 were obtained by cutting (Figure 2(b)) and were then grounded to a fine finished surface for macroetching. A solution composed of 50 pct HCl and 50 pct H$_2$O, at 50 °C, was used to reveal the macrosegregation patterns. Once the global macrosegregation patterns were detected, each block (Figure 2(b)) was cut into $2 \times 4 \times 7$ cm^3 smaller specimens (Figure 2(c)), which were used for detailed chemical analysis. A total of 910 samples were examined to develop an accurate chemical map of the slab. To this end, an ARL 4460 mass spectrometer especially equipped to analyze carbon concentration (detection levels below 100 ppm) was employed. In each case, three measurements were randomly performed and an average

Table I. Nominal Chemical Composition of the High-Strength Steel (Weight Percent)

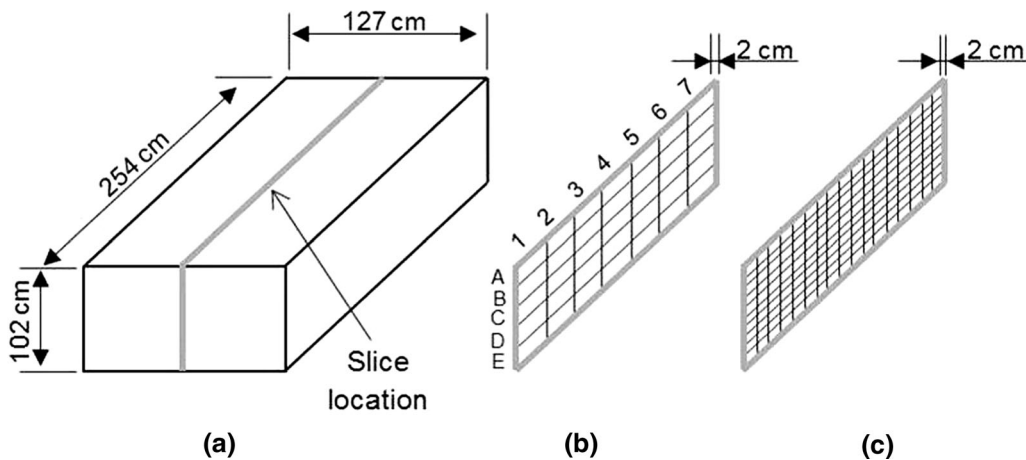| C	Mn	Ni	Cr	Mo	Si	Cu	P	S	Fe
0.35	0.99	0.5	1.86	0.53	0.40	0.15	0.014	0.004	balance

Fig. 2—Sample preparation: (a) slice location in the parallelepiped slab (forged and heat-treated ingot), (b) block cutting for macroetch, and (c) sample cutting for chemical analyses.

value was selected for the construction of the chemical map. The map was generated for each element listed in Table I.

III. MODELING OF A-TYPE MACROSEGREGATION PATTERNS

The quantification of the influence of deformation in modifying the A-type segregation pattern during forging was addressed using FORGE® NxT 1.1* software. The

---

*FORGE NxT 1.1 is a trademark of Transvalor S.A., France.

---

simulation reproduced, as close as possible, the actual industrial process sequences, including the following three sequences: (1) *upsetting*: the reduction of a cylindrical workpiece along its longitudinal axis[14]; (2) *free form Mannesmann* (*FM forging*): during which the top anvil is replaced with a platform, increasing friction upon contact and resulting in a more uniform deformation from the surface to the center; and (3) *cogging*: sequences of compressions applied along the length of the workpiece to reduce cross section and increase its length.[15]

Specifically, the upsetting, FM forging, and cogging sequences were simulated after each step so that the accumulated deformation was accounted as the starting point for the next step in the calculations. A 6-cm-diameter × 10-cm-length cylindrical specimen was chosen and built using CATIA V5 software to provide a three-dimensional geometry for simulation purposes. This particular initial geometrical form, with a considerable similarity to real industrial conditions, was selected in order to reduce calculation time while being able to produce significant, exploitable results and tendencies for the 40 MT ingot. The dies used for upset and FM forging were considered as infinite rigid plates, in accordance with the intermediate die used industrially for these forging sequences. However, in order to account for local effects of anvil geometry on ingot deformation, exact ratio scaled-down, upper, and lower anvil dimensions were used when simulating the cogging process. A chain simulation technique[16] was selected in order to correctly account for accumulated deformation in the workpiece. Finally, the material model developed in a previous study[17] was used as input data for simulating, as accurately as possible, the hot forging of the investigated alloy. Hydraulic press parameters and billet temperatures were supplied by an industrial partner. The billets were heated to 1260 °C before the forging operation, and the velocity of the upper die throughout forging stages changed from 2 to 15 mm/s.

Forging simulations were adapted to compute the grain flow throughout the part. The grain flow state variable[18] for multimaterial billets was applied for the modeling of A-type segregation. Planes of artificial fibers were selected as an edifice to visualize grain flow in the ingot core (Figure 3). The fibers representing grain flow, inserted into the diametric cross section, were
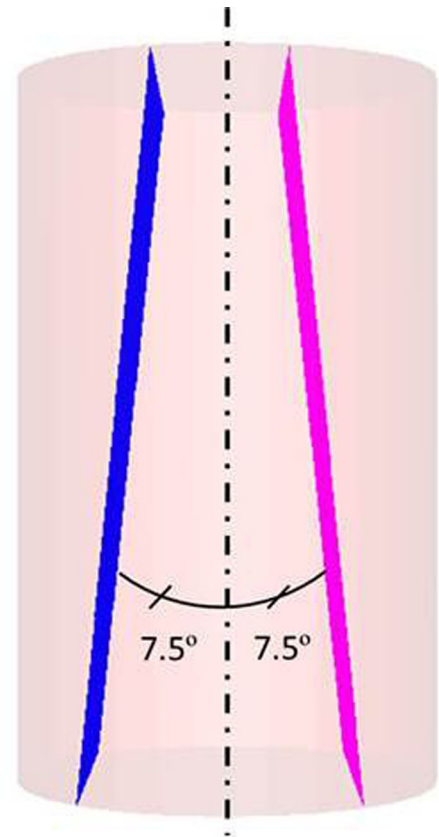

Fig. 3—Initial planes of artificial fibers oriented around ± 7.5 deg of the longitudinal axis of the ingot.

especially targeted. They correspond to observed segregation patterns in the large size cast ingots. Upon generation, initial plane orientation was specifically adjusted to around ± 7.5 deg of its principal axis (Figure 3) to match the observed as-cast A-segregate directions.[2] Initial boundary conditions for each of the following simulations in the chain used grain flow variation after deformation obtained from the previous sequence. The developed method ensures that the obtained results accurately account for the continuous forging process.

IV. RESULTS AND DISCUSSION

A. *Macroetch Analysis*

Due to the large dimensions of the examined slice, it is difficult to present a high-quality image of the macrosegregation patterns revealed by macroetch; therefore, they are indicated by arrows in Figure 4. These patterns, which have dark color, were observed on both sides 1 and 2 of the slab between its centerline and its external surface (Figure 4) and are composed of several continuous parallel bands (channels) that become discontinuous in the upper section of the slab. The observed patterns, especially the continuous ones, appear to be of A-type macrosegregation in agreement with those reported by other researchers.[1,3] The presence of dark

zones is often considered as an indication for the formation of positive segregation.[19] Also, it must be noted that no macrosegregation lines were detected in the centerline region.

Further examinations revealed that the continuous bands have a curved shape (wavy form), as illustrated in Figure 5, which corresponds to the region marked by
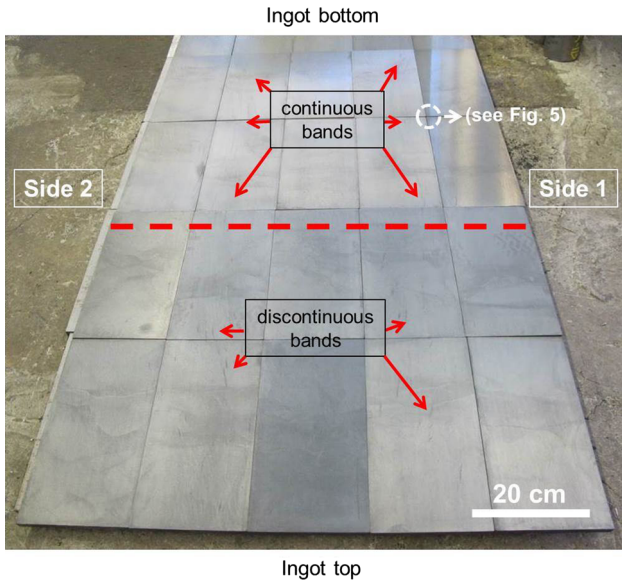

Fig. 4—A-type macrosegregation patterns revealed by macroetch (50 pct HCl and 50 pct H_2O at 50 °C) for the entire slice.
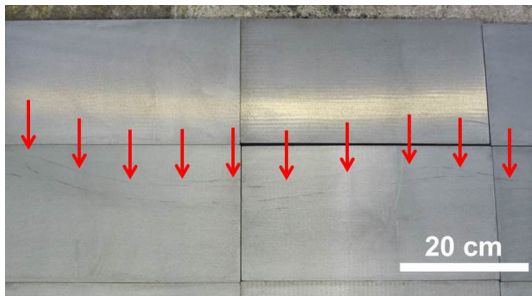

Fig. 5—Continuous curved (waved) channels of A-type macrosegregation patterns (zoom of the zone marked by white dashed circle from Fig. 4).

the white dashed circle in Figure 4. Figure 6 shows a schematic representation of typical curves for A-type macrosegregation in the forged ingot revealed by the macroetch experiments. Four macrosegregation zones from the bottom to the top of the slab were identified as follows:

(1) zone A1: located in the bottom of the slab and characterized without A-type macrosegregation patterns;
(2) zone A2: continuous A-type macrosegregation channels starting from each side 1 and 2 of the slab and developing until the typical A-type macrosegregation location (i.e., between the centerline and the outer surface of the slab);
(3) zone A3: continuous A-type macrosegregation bands located between the centerline and the outer surface of the slab (this region corresponds to the wavy pattern shape of Figure 5, and the channels on both sides are not really symmetric according to the longitudinal axis of the ingot); and
(4) zone A4: located in the upper part of the slab where the A-type macrosegregation lines become discontinuous.

It is well known that A-type macrosegregation bands are generally observed with linear shapes in the as-cast state[4] and that heat treatment is often unable to remove the global macrosegregation patterns due to required large diffusion distances.[20] The parallel lines in each side of the slab, observed in Figure 4, reflect the same shape, which could indicate that they have undergone similar deformation levels. Therefore, it is very important, from a process optimization point of view, to analyze and quantify the influence of deformation in modifying the segregation patterns during forging of large size ingots.

B. *Elemental Chemical Analysis*

Figure 7(a) shows a schematic representation of the distribution of carbon that allows identifying positive and negative macrosegregation zones over the entire surface of the slab. A detailed analysis of localized zones of positive and negative macrosegregations of different alloying elements was carried out and reported in a previous publication.[7] In addition, a third type of positive chemical heterogeneity pattern, present as
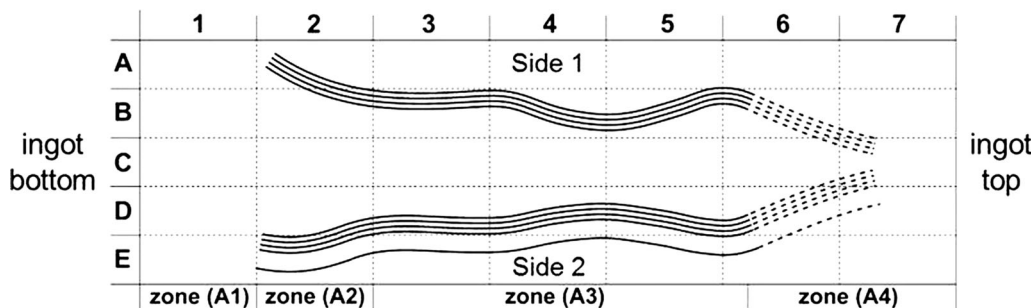

Fig. 6—Schematic representation of A-type macrosegregation patterns revealed by macroetch (50 pct HCl and 50 pct H_2O at 50 °C) for the entire slice.
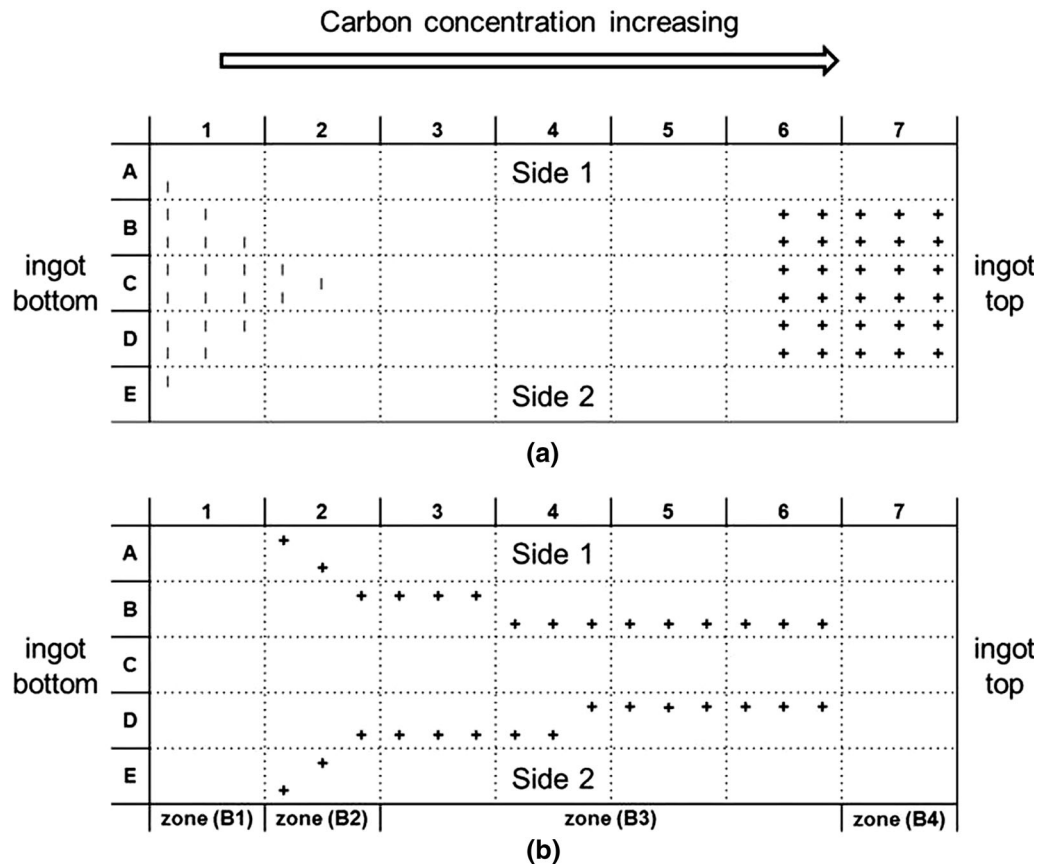
Fig. 7—Schematic representation of all macrosegregation patterns obtained by chemical analyses for carbon over the entire slice: (*a*) positive (negative) macrosegregation at the top (bottom) of the ingot and (*b*) A-type macrosegregation.

continuous bands (channels) and located between the centerline of the slab and its external surface, was observed (Figure 7(b)). These bands can be correlated with those observed after macroetch and associated with A-type macrosegregation. As indicated in Figure 7(b), carbon concentration in these bands is higher than its nominal value in the alloy and increases from the bottom to the top of the slab. Mass spectrometry results of the samples across the segregation bands and the zones immediately adjacent to them showed a difference in carbon concentration of the order of 0.07 wt pct. In order to simplify the analysis of A-type macrosegregation patterns, four different zones (Figure 7(b)) were identified as follows:

(1) zone B1: located in the bottom of the slab and characterized without A-type macrosegregation;
(2) zone B2: A-type macrosegregation channels starting from the external surface of each side of the slab and developing between the centerline and the external surface;
(3) zone B3: A-type macrosegregation patterns present between the centerline of the slab and its external surface (each slab side is composed only with one straight line that undergoes a shift in its position, and the two channels are not symmetric according to the longitudinal axis of the ingot); and

(4) zone B4: absence of continuous and discontinuous bands of the A-type macrosegregation patterns.

The boundaries of A-type macrosegregation patterns were revealed by macroetch and confirmed by chemical analysis. Both techniques show the nonsymmetry of A-type macrosegregation patterns according to the longitudinal axis of the ingot and the existence of the same number of zones. Zones A1 and B1, which are located in the bottom of the slab, do not present any A-type macrosegregation patterns. Also, both zones A2 and B2 show starting regions of A-type macrosegregation. However, the A-type macrosegregation patterns revealed in zones A3 and B3 do not present the same morphology. It should be noted that the wavy and parallel bands of A-type macrosegregation revealed by macrotech do not correspond *exactly* to those revealed by chemical mapping. These differences could be due to the difference in the accuracy level of each technique and the possible presence of large zones of positive segregation with similar composition to the A-type, thereby rendering difficult the distinction of the exact form of A-type macrosegregation. Furthermore, discontinuous bands detected in zone A4 are not clear in zone B4, where no A-type macrosegregation patterns are observed. In contrast, zone B4 is characterized by positive segregation, which could interfere with A-type

bands. However, different strain paths during forging could also affect the shape of the continuous bands. Finally, it should be noted that A-type segregation patterns clearly show manganese and chromium enrichment. Cao et al.[11] also reported the presence of carbon, silicon, and manganese in A-type macrosegregation, thereby confirming enrichment by alloying elements in this type of macrosegregation.

C. Primary Solidification Mode

The existence and extent of A-segregation are dependent on the chemical composition of the steel.[21] So, the presence of carbon, manganese, and chromium in the A-type segregation is indicative of the possible interaction between these elements, which could affect their segregation behavior. Specifically, Dhindaw et al.[22] reported that the presence of carbon and its interaction with chromium and molybdenum causes important changes in the equilibrium distribution coefficient and can lead to significant levels of macrosegregation. Indeed, carbon with its low partition coefficient in steel has a strong tendency to segregate during solidification.[23] Because its solubility in the solid is lower than that in the liquid, it will be rejected into the melt and, therefore, high propensity for segregation is produced.[5] The rejection of carbon, or another solute, results in

changes in the chemical composition of the liquid metal during the solidification process. This compositional change may affect the steel's primary solidification mode (δ-ferrite or austenite), which can, in turn, affect the segregation range of the various alloying elements.[24]

In order to identify the main solidification mode, calculations of the phase fractions of δ-ferrite, austenite, and liquid vs temperature were performed using THERMO-CALC software for one sample from within the A-type segregation band and one from outside the band. Table II presents the chemical compositions of both samples, where it can be seen that carbon is the solute element presenting the main difference, around 0.07 wt pct. The results shown in Figure 8 indicate that for both samples, δ-ferrite is the first formed phase, though with a very low fraction for the sample taken from the A-type band. Thus, an increase in carbon concentration will probably result in nil δ-ferrite fraction during the primary austenitic solidification stage. The preponderance of this solidification mechanism will probably affect the segregation behaviors of the other elements, as discussed subsequently. The primary solidification mode in δ-ferrite implies a peritectic transformation to austenite and, therefore, a more complicated microsegregation pattern. During primary solidification and the peritectic transformation, carbon tends to diffuse out of δ-ferrite in order to form austenite,

Table II. Chemical Composition of (a) Sample Selected Nearly A-Type Segregation Region and (b) Sample Selected from A-Type Segregation Band (Weight Percent)

Sample	C	Mn	Ni	Cr	Mo	Si	Cu	P	S	Fe
(a)	0.38	0.93	0.52	1.76	0.47	0.38	0.15	0.013	0.003	balance
(b)	0.45	0.95	0.52	1.76	0.48	0.39	0.15	0.013	0.003	balance
ΔX^*	0.07	0.02	0	0	0.01	0.01	0	0	0	0

ΔX^*: difference of chemical composition between the samples (a) and (b).

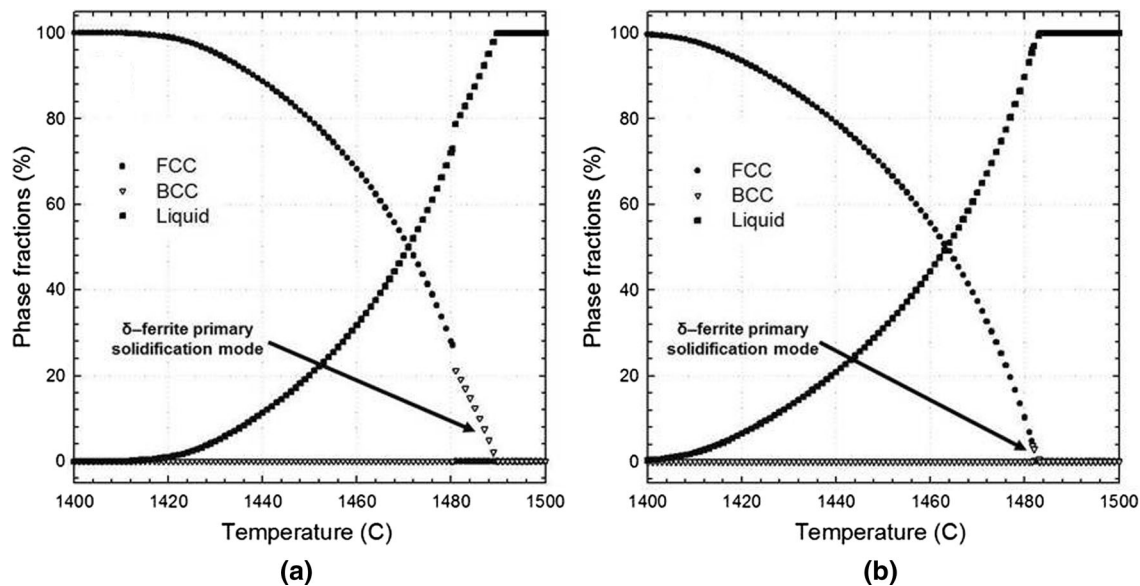Fig. 8—Phase fraction evolutions, as a function of temperature, of δ-ferrite, austenite, and liquid, showing the primary solidification mode for (a) sample selected from nearly A-type segregation region and (b) sample selected from A-type segregation band.
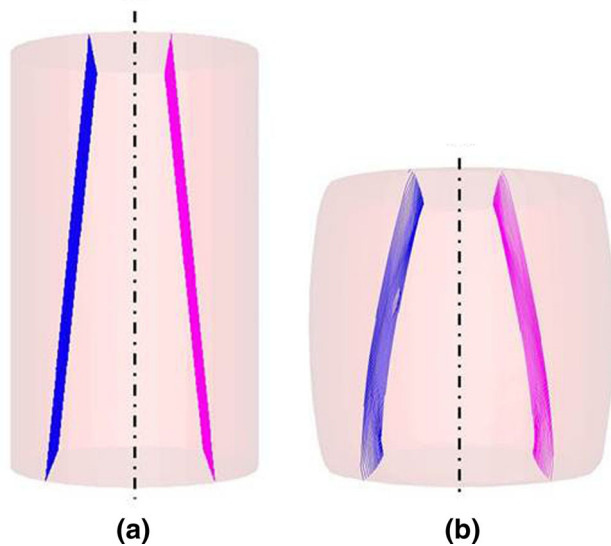
Fig. 9—Grain flow deviation (*a*) before and (*b*) after the upsetting.

Fig. 10—Grain flow deviation (*a*) before and (*b*) after the FM effect.

whereas the chromium remains in the structure and will not diffuse to austenite.[22] Due to the limited diffusion of chromium, its tendency to segregate is significantly reduced.

D. Simulation of Forging Effect on A-Type Macrosegregation Patterns

Figures 9 through 11 show grain flow deviation after the upsetting, FM, and cogging sequences, respectively. Individual observations of the consecutive ingot forging sequences prove that the mechanism for wave formation is gradual and, therefore, can be broken down into a sequential structure. The first major material deformation occurs during upsetting (Figure 9(b)). The A-type segregation undergoes bowing, also referred to as ''cowboy-leg formation.'' The bowing is mainly observable along the vertical axis (front view) but is also present to a much lesser degree around the diameter. The severity of the grain flow bowing effect is determined by the reduction percentage during upsetting. In accordance with industrial practices, the simulated ingot was reduced by 68 pct. The influence of bowed macrosegregation can be measured by comparison with initial plane orientation. The most affected A-segregates, located around one third of the ingots' final height, measure 14.7 deg in relation to the vertical axis (Figure 9(b)). This value is nearly twice that of the initial plane orientation (Figure 9(a)). The location corresponding to maximal bowing severity from upsetting is essential to wave formation in the following forging sequences, as it constitutes the meeting point for the two developed wave fronts.

Wave formation along the ingots' principal axis becomes apparent as the second major deformation takes place (Figure 10). However, due to the orientation of the workpiece during the FM process, bowing in relation to the ingots' secondary axis (end view) is revealed to be more prominent. This also shows the effect of the
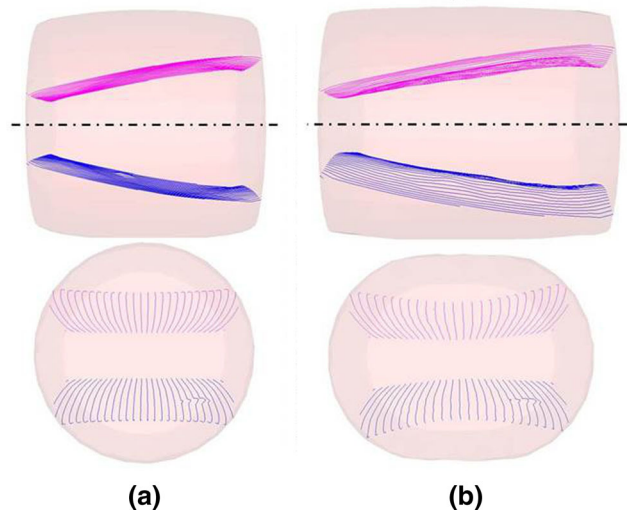
variation of the forging direction on grain flow and deformed A-segregates found on a diametric plane. Wave formation takes place in the ensuing sequences (Figure 11). The FM forging and cogging sequences both modify the amplitude of the crests but do not significantly change the form of the double-crested A-segregate wave pattern. In this case, the FM process creates two waves, each with two crests (Figure 12). The amplitude of the crest created below the maximal bowing severity location for upsetting (initial lower third of the billet) is superior to that from above, $d_2 > d_1$ and $d_4 > d_3$. The orientation of the initial A-segregates in regard to the face being forged during the FM process favors the formation of the wave whose curvature is toward the mobile anvil from the hydraulic press (in this case, the lower blue wave), $d_3 > d_1$ and $d_4 > d_2$. However, the ratio between in-wave crest amplitudes remains constant at this part in the forging process, $r_{FM} = d_2/d_1 = d_4/d_3 = d_3/d_1 = d_4/d_2 \sim 1.3$. This indicates that the forging effects on A-segregates are not symmetrical but are constant throughout the ingot.

A constant increase of 5, 6, and 7 pct was observed between crest amplitudes before and after wave definition, d_{FM} and $d_{cogging}$, for d_1, d_3, and d_4. However, a variation of 19 pct was noted for d_2. An increase in amplitude was present for all crests, proving that the cogging sequence defines and magnifies the deformation of the A-type segregation lines. The calculation of the in-wave ratio, $r_{cogging}$, varied between 1.1 and 1.5, indicating the absence of symmetry and homogenous behavior in the geometry of the ingot and the effects of the forging process on the segregation lines. It can be seen that deformation from the open die forging process has significantly affected the morphology of the A-type segregates initially observed. The simulations predict a wavy shape, as revealed by macroetch (Figure 5). Good correlation between tendencies can be seen through the simulated and experimental results. Bowing occurs during upsetting and the waves appear after the FM forging sequence. Amplitude and profiles of individual waves are then tailored by the cogging sequence. The
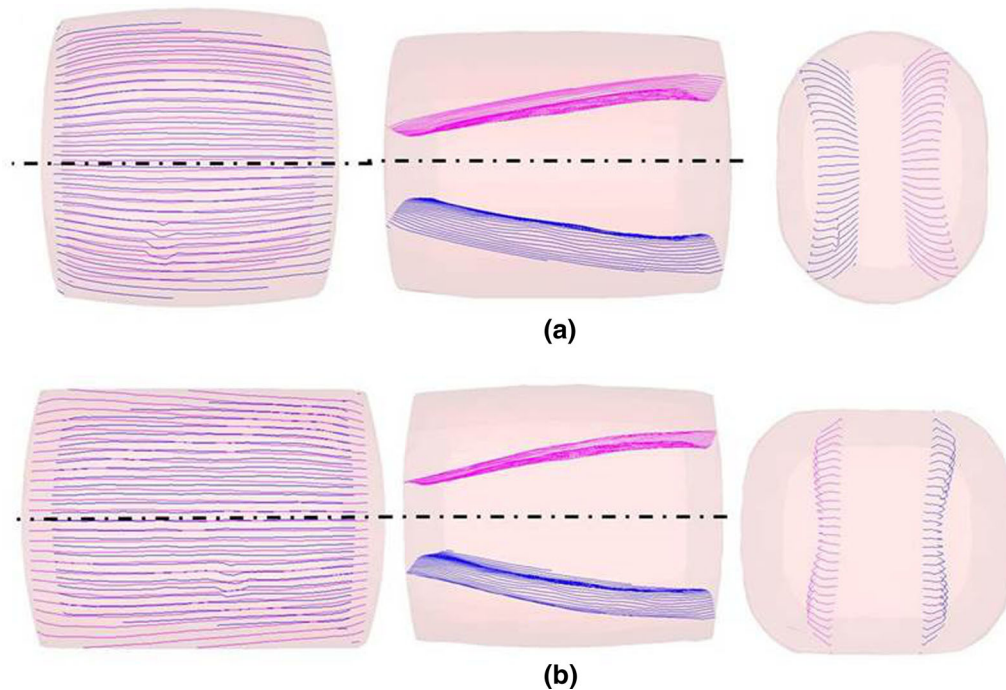
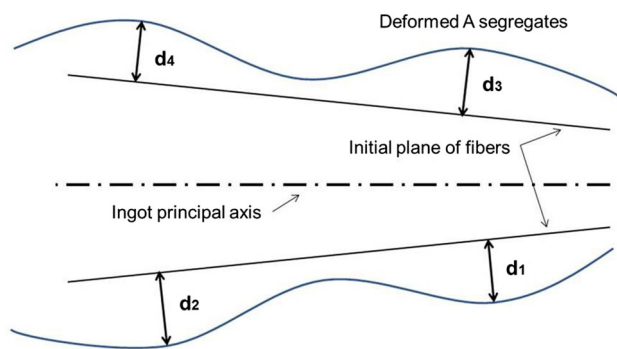Fig. 11—Grain flow deviation (*a*) before and (*b*) after the cogging.

Fig. 12—A-segregate deformation schematic.

developed model seems to be a very useful tool to predict the evolution of A-type macrosegregation patterns during the thermomechanical process.

V. CONCLUSIONS

The present study was undertaken with the view to analyze the A-type macrosegregation pattern of different alloying elements and to investigate the effects of forging and heat treatment operations on this pattern in a large size forging of high-strength steel through experimentation and modeling. The results show that A-type segregation occurs on both sides of the slab; was enriched in carbon, manganese, and chromium; and could affect the primary solidification mechanism of steel. Good agreement between the finite element modeling simulation predictions and experimental observations was demonstrated. The observed wave formation of the macrosegregation patterns was analyzed in the simulation and related to thermomechanical processing parameters. The wave formation mechanism was found to be sequential and analysis was proposed to discretize it in three steps: initial bowing, wave formation, and wave definition.

REFERENCES

1. G. Lesoult: *Mater. Sci. Eng., A,* 2005, vols. A413–A414, pp. 19–29.
2. M. Wu, J. Li, A. Kharicha, and A. Ludwig: in *Proc. 2013 Int. Symp. on Liquid Metal Processing & Casting,* Austin, TX, M.J.M. Krane, A. Jardy, R.L. Williamson, and J.J. Beaman, eds., 2013, pp. 171–80.
3. J.J. Moore and N.A. Shah: *Int. Mater. Rev.,* 1983, vol. 28, pp. 383–56.
4. Y.F. Cao, Y. Chen, and D.Z. Li: *Acta Mater.,* 2016, vol. 107, pp. 325–36.
5. M.T. Rad, P. Kotas, and C. Beckermann: *Metall. Mater. Trans. A,* 2013, vol. 44A, pp. 4266–81.
6. E.J. Pickering and H.K.D.H. Bhadeshia: *J. Press. Vess. Technol.,* 2014, vol. 136, pp. 031403-1–031403-7.
7. A. Loucif, E. Ben Fredj, M. Jahazi, L.-P. Lapierre-Boire, R. Tremblay, and R. Beauvais: *Proc. 6th Int. Congr. on the Science and Technology of Steelmaking (ICS2015),* Beijing, 2015, pp. 1043–46.
8. J. Miettinen: *Metall. Mater. Trans. B,* 1997, vol. 28B, pp. 281–97.

9. B. Santillana, R. Boom, D. Eskin, H. Mizukami, M. Hanao, and M. Kawamoto: *Metall. Mater. Trans. A*, 2012, vol. 43A, pp. 5048–57.
10. A. Olsson, R. West, and H. Fredriksson: *Scand. J. Metall.*, 1986, vol. 15, pp. 104–12.
11. Y.F. Cao, Y. Chen, P.X. Fu, H.W. Liu, and D.Z. Li: *Metall. Mater. Trans. A*, 2017, vol. 48A, pp. 2260–73.
12. E.J. Pickering, C. Chesman, S. Al-Bermani, M. Holland, P. Davies, and J. Talamantes-Silva: *Metall. Mater. Trans. B*, 2015, vol. 46B, pp. 1860–74.
13. H. Ge, F. Ren, J. Li, X. Han, M. Xia, and J. Li: *Metall. Mater. Trans. A*, 2017, vol. 48A, pp. 1139–50.
14. M.P. Groover: *Fundamentals of Modern Manufacturing: Materials, Processes and Systems*, 4th ed., Wiley, New York, 2010, pp. 406–407.
15. W.L. Zhao and Q.X. Ma: *Mater. Trans.*, 2015, vol. 56, pp. 850–57.
16. N. Harris, D. Shahriari, and M. Jahazi: *J. Manuf. Process.*, 2017, vol. 26, pp. 131–41.
17. K. Chadha, D. Shahriari, and M. Jahazi: *Metall. Ital.*, 2016, vol. 4, pp. 5–12.
18. FORGE NxT 1.0®, Transvalor S.A., Cedex, France.
19. B. Sang, X. Kang, and D. Li: *J. Mater. Process. Technol.*, 2010, vol. 210, pp. 703–11.
20. E.J. Pickering: *ISIJ Int.*, 2013, vol. 53, pp. 935–49.
21. K. Suzuki and K. Miyamoto: *Trans. ISIJ*, 1978, vol. 18, pp. 80–89.
22. B.K. Dhindaw, T. Antonsson, J. Tinoco, and H. Fredriksson: *Metall. Mater. Trans. A*, 2004, vol. 35A, pp. 2869–79.
23. G.E. Totten, L. Xie, and K. Funatani: *Handbook of Mechanical Alloy Design*, Marcel Dekker Inc., New York, 2014, pp. 133–34.
24. M. Fujda: *JMMM*, 2005, vol. 15, pp. 45–51.